Inhomogeneous diffusion-limited aggregation

Robin Blumberg Selinger
Center for Polymer Studies and Department of Physics, Boston University, Boston, Massachusetts 02215 and Lyman Laboratory of Physics, Harvard University, Cambridge, Massachusetts 02138

Johann Nittmann
Digital Equipment Corporation, Campus-based Engineering Center, 7 Favoritenstrasse 7, 1040 Vienna, Austria

H. E. Stanley
Center for Polymer Studies and Department of Physics, Boston University, Boston, Massachusetts 02215
(Received 19 September 1988)

In order to simulate viscous fingering in a porous medium with inhomogeneous permeability, we make use of a generalization of the diffusion-limited aggregation (DLA) model. In this generalized DLA, the randomly diffusing particles have transition probabilities which depend on the local permeability values of the underlying medium. This method is applied to the simulation of unstable two-fluid displacement in two-dimensional disordered pore-pipe networks. We show that the model may only be used to simulate flow in media which have inhomogeneous permeability and homogeneous porosity. We explore the combined effects of two types of noise: noise in the growth process, and disorder in the permeability of the medium; we find a morphology phase diagram which shows that both types of noise strongly affect morphology selection. In addition, we perform an analysis of DLA with noise reduction and find that the magnitude of interface velocity fluctuations is proportional to $1/\sqrt{s}$, where s is the noise-reduction parameter. We show that these fluctuations are "multiplicative" in character and vanish in the large-noise-reduction limit. Finally, we address the potential application of this model to petroleum reservoir simulation.

I. INTRODUCTION

The phenomenon of viscous fingering in porous media[1-7] has received much attention because it is related to the class of fractal growth processes that includes dielectric breakdown,[8] dendritic crystal growth,[9] and diffusion-limited aggregation (DLA).[10] Viscous fingering is also of practical interest because it is involved in enhanced oil recovery. Paterson[11] first proposed that DLA may be used to model two-fluid displacement if the driving fluid is inviscid, the displaced fluid is Newtonian, and wetting effects and surface tension are negligible. In this work we address the problem of flow under these conditions in an inhomogeneous medium, neglecting the effects of dispersion.

Paterson[12] also showed that two-fluid displacement in a porous medium with *inhomogeneous* permeability may be modeled by DLA if the lattice constant in the DLA system is taken to be proportional to the local permeability. This variant of DLA works only for geometries in which the permeability varies by blocks or layers, but it does not work if the permeability is disordered. If the permeabilities of the bonds in a two-dimensional square network are chosen randomly, the corresponding lattice with random lattice constants does not generally lie in the plane. Thus, Paterson's variant of DLA cannot be used for simulating viscous fingering in disordered systems.

Meakin[1] introduced a generalization of DLA in which an incident diffusing particle has transition probabilities which depend on the local permeabilities. We refer to this model as inhomogeneous diffusion-limited aggregation, or IDLA. Siddiqui and Sahimi[13] considered IDLA independently and applied it to the simulation of two-fluid displacement in two-dimensional inhomogeneous porous media. Here we explore the details of the mapping between IDLA and the fluid-flow problem, and introduce a coarse-graining step that dramatically increases the computational efficiency of the IDLA model. We also investigate the effects of "noise reduction"[14-17] on DLA in general, and study the interaction between noise in the IDLA growth process and disorder in the medium. We hope that this interaction may share at least some characteristics with the interaction between the two types of noise that are important in viscous fingering: fluctuations at the unstable fluid boundary and disorder in the permeability of the porous medium. In addition, we find that the magnitude of interface velocity fluctuations is proportional to $1/\sqrt{s}$, where s is the noise-reduction parameter. We show that these fluctuations are "multiplicative" in character and vanish in the large noise-reduction limit.

It should be noted that the IDLA model is closely related to the dielectric breakdown model (DBM),[8] where the permeability may be interpreted as a local dc conductivity. Because the IDLA model does not require the repeated solution of the governing equations, it is more efficient computationally than DBM. Nittmann and Stanley[15] simulated viscous fingering in a medium with permeability that varied in a layered fashion by using the DBM.

Oxaal *et al.* and others[6] have also used the DBM to study viscous fingering in one special type of porous

medium, a percolation cluster. In such a medium, a fraction p_c of the medium has permeability $k=1$, while the remaining fraction $1-p_c$ has permeability $k=0$. Regions of the two permeabilities are distributed randomly. Here, p_c is the percolation threshold for the lattice under consideration. In the present work, we consider a more general case, in which the permeabilities of the bonds in the entire network take on arbitrary values, and fluid flow is not restricted to a percolation cluster. Sahimi and Siddiqui[7] simulated miscible viscous fingering on percolation clusters in which the channels of the clusters have randomly distributed radii and pointed out that there may be important differences between the DLA model and miscible viscous fingering in inhomogeneous media. In the present work we demonstrate that the DLA model can only be mapped onto viscous fingering in a medium with inhomogeneous permeability and homogeneous porosity. A pore-pipe network is an example of such a medium, as shown below. Because Sahimi and Siddiqui compared DLA with a simulation of viscous fingering in a network of pipes, which has inhomogeneous porosity, our finding perhaps explains the discrepancies they found between the two.

In the next section we address the detailed mapping between the IDLA model and fluid flow in porous media, and introduce a coarse-graining step. This coarse graining increases the computational efficiency of the algorithm by allowing walkers to take large steps when far from the cluster. In Sec. III we discuss the experiments and simulations of Chen and Wilkinson[3] on a disordered network of capillaries. In Sec. IV we present an analysis of the effects of noise reduction on DLA, or on any other growth process in general, and explore the combined effects of noise in the DLA growth process and disorder in the medium. In Sec. V we summarize our results, and discuss the possibility of adapting a DLA-based model further for use in simulating fluid flow in a petroleum reservoir. In the Appendix we present a more detailed analysis of the mapping between IDLA and flow in disordered porous media.

II. THE IDLA MODEL AND THE IDEALIZED POROUS MEDIUM

Consider an idealized porous medium consisting of a square lattice of pores of uniform volume, connected by narrow cylindrical channels, or pipes. The pipes are of uniform length L, but their radii vary in size, as shown in Fig. 1. We assume that the volume of the pipes is negligible compared to that of the pores. In a pipe of radius r, incompressible viscous fluid flows according to the Poiseuille law,

$$\mathbf{Q}=-\left[\frac{\pi r^4}{8\mu}\right]\nabla P \ . \tag{2.1}$$

Here, $\mathbf{Q}$ is the volume flow rate, μ the viscosity, and ∇P is the pressure gradient along the pipe. If incompressible fluid is flowing through the medium, then

$$\nabla\cdot\mathbf{Q}=0 \ . \tag{2.2}$$

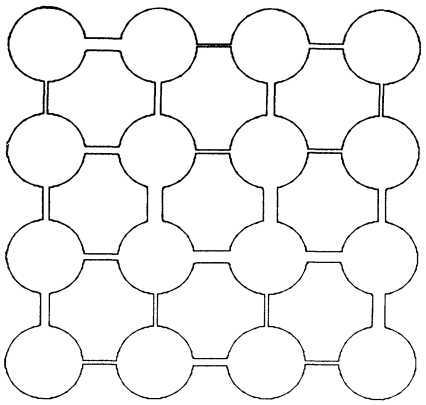

FIG. 1. An example of a pore-pipe network.

Substituting (2.1) into (2.2) produces

$$\nabla\cdot(K\nabla P)=0 \ , \tag{2.3}$$

where the conductance K has the form

$$K=\frac{\pi r^4}{8\mu} \ . \tag{2.4}$$

In our discretized description, P is defined on the pore sites, which are at the vertices of the lattice, while K is defined on the pipes, which are the bonds of the lattice. We take continuum differential operators to represent their discretized analogs.

Darcy's law states that

$$\mathbf{v}=-k\nabla P \ , \tag{2.5a}$$

where $\mathbf{v}$ is fluid velocity and k is permeability, also defined on the bonds of the lattice. For flow in a cylindrical pipe, $\mathbf{v}=\mathbf{Q}/\pi r^2\sim r^2\nabla P$ and thus $k\sim r^2$.

However, in the case of the pipe and pore network as described above, the magnitude of the effective fluid velocity $\mathbf{v}$ is

$$\mathbf{v}=\mathbf{Q}a/V \ , \tag{2.5b}$$

where a is the lattice spacing between pores and V is the uniform volume of each pore. That is, the velocity is proportional to the flow rate, and thus the effective permeability of the medium is $k\sim r^4$. Note that according to Eq. (2.4) the conductance $K\sim r^4$ also. This proportionality between k and K is necessary in order to map the fluid-flow problem onto the IDLA model. That is, the K in Eq. (2.3) must be proportional to the k in Darcy's law, Eq. (2.5a), and this is only possible if the fluid velocity is proportional to the flow rate. For many systems, there is no such equivalence, e.g., a system of pipes without pores, for which $\mathbf{v}=Q/\pi r^2$ and thus $K\sim r^4$ and $k\sim r^2$. For such a system, *there is no simple map onto a DLA-based model.* Thus, the IDLA model is applicable to two-fluid displacement only in media such as the pipe-pore network; that is, media which have constant porosity and inhomogeneous permeability.

This important detail of the mapping between IDLA and fluid flow in porous media perhaps explains the

disagreement found by Sahimi and Siddiqui[7] between the fractal dimension of DLA on a percolation cluster and that of simulated viscous fingering patterns in a porous medium which consists of a percolation cluster in which the channels of the cluster have randomly distributed radii. Since there is no mapping between the two systems, there is no reason for the fractal dimensions to be the same.

Now consider a viscous fingering experiment with infinite viscosity ratio and no surface tension. At the outset, the entire pipe and pore network is filled with viscous fluid. The inviscid ($\mu=0$) fluid is then injected at one pore site. Within the injected fluid, the pressure P is constant, while the pressure in the displaced fluid obeys Eq. (2.3). In the absence of surface tension, the interface between the fluids is at constant pressure. Boundary conditions at the edge of the pore-pipe system are, (i) for an open boundary, $P=P_{\text{atmosphere}}$, and (ii) for a closed boundary, $\nabla P\cdot\mathbf{n}=0$, where $\mathbf{n}$ is the unit normal to the boundary.

The fluid interface proceeds according to Eq. (2.5a), with the normal velocity

$$v_n=-k\nabla P\cdot\mathbf{n}\ . \tag{2.6}$$

In the case of a homogeneous system, where all pipes have the same radius, Eq. (2.3) reduces to the Laplace equation

$$\nabla^2 P=0\ . \tag{2.7}$$

The pressure in a smooth Hele-Shaw cell also obeys Eq. (2.7).

Now we turn to the mapping between viscous fingering and DLA. The DLA model begins with a "seed" cluster of one particle placed at the center of a circle. Another particle is released from a randomly chosen location on the circle and performs a random walk. If it returns to the circle, the particle is destroyed. If it arrives at the cluster, it sticks at the point of contact and becomes part of the cluster. In either case, another particle is then released from a newly chosen random position on the circle. In this way the cluster grows as particles aggregate one by one.

The analogy between viscous fingering in smooth Hele-Shaw cells and DLA was first pointed out by Paterson,[11] who showed that Eq. (2.7) is identical to the diffusion equation for random walkers in steady state,

$$\nabla^2 u=0\ . \tag{2.8}$$

Here, u is the particle probability density, and it plays the role of pressure. The probability p_{hit} that a particle will hit the cluster at a given point along its perimeter is

$$p_{\text{hit}}\sim\nabla P\cdot\mathbf{n}\ . \tag{2.9}$$

This equation is analogous to that for the finger interface normal velocity, Eq. (2.6). A discussion of this analogy is given in the Appendix.

To find a generalization of DLA which models flow in *inhomogeneous* media, it is necessary to find a random-walk process which yields a diffusion equation in steady state identical in form to (2.3). One such random-walk process is a *generalized* form of the "blind ant" walk.[18] For simplicity, we begin by discussing a one-dimensional system; the extension to two or more dimensions is straightforward. Consider a one-dimensional lattice of sites connected by bonds, where k_i is the permeability of bond i (see Fig. 2). We may consider any set of values of k_i that we wish. In order to study a disordered medium, one might choose the values of the k_i randomly according to some probability distribution. In order to choose an appropriate time unit, the k_i are normalized such that $0\le k_i\le 1/z$, where z is the coordination number of the lattice. The walk process is discretized in both time and space. Let $\omega_{i,j}$ be the probability per unit time for a walker at site i to step to site j. The *generalized* blind ant rules are

$$\omega_{i,i+1}=k_i\ ,$$
$$\omega_{i,i-1}=k_{i-1}\ , \tag{2.10}$$

and

$$\omega_{i,i}=1-k_i-k_{i-1}\ .$$

That is, the random walker is biased toward high-permeability bonds, and the probability to step along a bond is equal to the permeability of that bond. The normalization of the k_i ensures that the probabilities are non-negative.

From (2.10), the discrete diffusion equation for this walk process is

$$u(i,t+1)=u(i+1,t)k_i+u(i-1,t)k_{i-1}+u(i,t)(1-k_i-k_{i-1})\ . \tag{2.11}$$

Here $u(i,t)$ is the probability density of a diffusing particle. Equation (2.11) may be rearranged as follows:

$$u(i,t+1)-u(i,t)=[u(i+1,t)-(i,t)]k_i-[u(i,t)-u(i-1,t)]k_{i-1}\ , \tag{2.12}$$

which is a discretized form of

$$\frac{du}{dt}=\frac{d}{dx}\left[k\frac{d}{dx}u\right]\ . \tag{2.13}$$

If these rules are generalized to two or three dimensions, then the diffusion equation becomes

$$\frac{du}{dt}=\nabla\cdot(k\nabla u)\ , \tag{2.14}$$

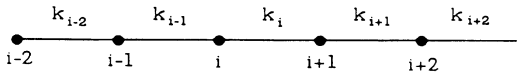

FIG. 2. The one-dimensional system of sites connected by bonds, where k_i is the permeability of the bond between sites i and $i+1$.

which in steady state reduces to (2.3). Thus, to simulate flow in a medium with spatially varying permeability, it is sufficient to carry out a DLA simulation where the diffusing particles obey the generalized blind ant rules. That is, in IDLA we begin by assigning a permeability to every bond in a lattice according to any rule we wish. Then we place a one-site seed cluster in the center of a large circle on the lattice. A random walker is released at a randomly chosen position on the circle and diffuses according to the rule that the transition probability from one site to another is equal to the normalized permeability of the bond between. If the walker returns to the circle, it is destroyed and a new walker is launched from a new random location on the circle. If a walker reaches the cluster, it sticks at the point of arrival and a new walker is launched from a new random location on the circle. These rules define the IDLA model. A more complete discussion of the mapping between IDLA and the fluid-flow problem is given in the Appendix.

We introduce two important alterations to the IDLA model which greatly increase its efficiency. First, we change the transition probabilities slightly in order to accelerate each walker's progress along its trajectory. According to the generalized blind ant rules, a walker can be temporarily trapped in any area of very low permeability, as it can wait at the same site for many time steps. Because the only important attribute of each walker's trajectory is its endpoint, it is possible to speed up the determination of the trajectory by setting the probability for a walker to stay at the same site to 0, and then normalizing the probabilities to step to the neighbor sites. Thus walkers move more efficiently through low-permeability areas. Referring again to Fig. 2 for the one-dimensional case, we see that the accelerated rule is

$$\omega_{i,i+1}=\frac{k_i}{k_{i-1}+k_i}$$

and (2.15)

$$\omega_{i,i-1}=\frac{k_{i-1}}{k_{i-1}+k_i}\ .$$

This set of rules corresponds to a *generalized* myopic ant walk.[18] The generalization to two dimensions is straightforward: the transition probability from site i to site j is equal to the permeability of the bond between, divided by the sum of the permeabilities of the four bonds touching site i. Using these accelerated transition probabilities is not an approximation, but simply a convenient way to increase the efficiency of the simulation. (Note: the boundary condition at the outer circle implies that a walker's first step from the boundary must be made according to the original rule, not the accelerated rule, as it has a finite probability of staying on the circle and thus being destroyed.)

The second alteration to the model to increase its efficiency is a coarse graining of the permeabilities. This approximation makes it possible for random walkers to take steps of a size larger than the lattice constant. Such a coarse graining is only appropriate if the underlying permeabilities do not have any special spatial correlations which might be destroyed by a coarse graining. We begin with a realization of an $n\times n$ square lattice of bonds. The permeability of each bond is assigned by a rule of our choice. Now we cut the lattice into $(m\times m)$-sized squares, where m is much smaller than n. We numerically solve Eq. (2.3) on each $m\times m$ square with $P=1$ on the top boundary, $P=0$ on the bottom boundary, and $\nabla P\cdot\mathbf{n}=0$ on the side boundaries. The current $k\nabla P$ is summed along the top boundary of each square, and this current is taken to be the permeability of a vertical bond in the $(n/m)\times(n/m)$ coarse-grained permeability lattice. Thus each $m\times m$ square is reduced to a single vertical bond in the coarse lattice. The original lattice is again partitioned into $m\times m$ squares (displaced by $m/2$ to the right from the first set) and the process is repeated, except that the boundary conditions are rotated by 90°, so that horizontal permeabilities are calculated. The displacement of the second partitioning to the right ensures that the horizontal bonds join with the vertical bonds to form a square lattice of coarse-grained permeabilities.

With this coarse graining, each walker is released at the outer circle and walks according to the usual IDLA rules on the coarse lattice, thus making steps of length m lattice constants. When it comes to a site near—within $3m$ lattice constants—to any cluster site, then it switches to walking on the original lattice, starting at a randomly chosen position in the $m\times m$ square enclosing the coarse lattice site. If it returns to a region far from any cluster site, then it returns to walking on the coarse lattice.

This technique tremendously increases the efficiency of the IDLA algorithm and thus allows us to produce clusters of 10 000–20 000 particles in 5–10 min of IBM 3090 CPU time. However, there is the danger that the approximation will wash out some important details of the medium, as some paths through the permeability lattice are always neglected in the coarse graining. In this work we have mostly studied lattices of size approximately 500×500 partitioned into 10×10 units, such that the coarse lattice is of size 50×50. No differences were found between clusters made with and without the coarse-graining procedure at this level. If the coarse-graining length were too large, then the medium would appear to be uniform regardless of the permeability configuration.

In "DBM"-type boundary conditions, a random walker must step onto a cluster site before "sticking" to the aggregate. Kadanoff[19] concluded that DBM-type boundary conditions[8] are better suited to simulations of viscous fingering than DLA-type boundary conditions.[10] This is the boundary condition used in all the simulations presented here.

To demonstrate that IDLA is equivalent to the related models discussed above, we have generated clusters under conditions similar to those in the references for comparison, and find good agreement. One example of an IDLA simulation carried out in the quarter-five-spot geometry considered by Paterson[12] is shown in Fig. 3. The middle section has a permeability half that of the surrounding area. Comparison with Fig. 5 of Ref. 12 shows that the IDLA model appears to be equivalent to Paterson's variant of DLA for this simple geometry.

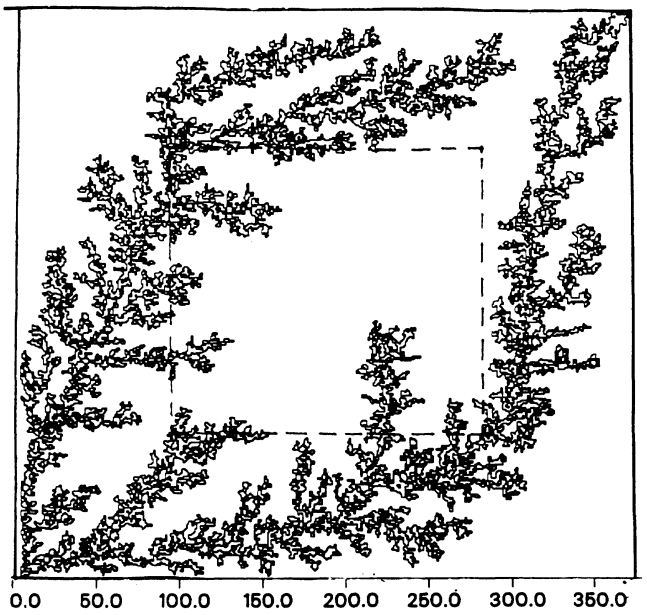

FIG. 3. An IDLA simulation with no noise reduction ($s=1$) for a two-dimensional 390×390 square lattice in the quarter-five-spot geometry. The inner region has permeability half that of the outer region. This figure may be compared with Fig. 5 of Ref. 12. The cluster perimeter shown here corresponds to the boundary of filled pores in a pipe-pore network.

III. VISCOUS FINGERING IN TWO-DIMENSIONAL DISORDERED PIPE NETWORKS

Chen and Wilkinson[3] (CW) studied viscous fingering in two-dimensional disordered pipe networks both experimentally and theoretically. In their simulations, they treat a system consisting of a square lattice of cylindrical pipes with fixed length L, but with radii r distributed uniformly in the interval $[1-\lambda, 1+\lambda]$. Here, $L \gg 1+\lambda$ and $0 \le \lambda \le 1$. The adjustable parameter λ controls the disorder of the network: $\lambda=0$ corresponds to a homogeneous system, while $\lambda>0$ corresponds to an inhomogeneous system.

In their experiments, CW found a transition from a dendritic morphology for small λ to a more DLA-like morphology for large λ. While the pipe network studied by CW is not identical to the pipe-pore system modeled by IDLA, it seems likely that they will at least share qualitative features.

Siddiqui[13] simulated IDLA on such a system without noting that the mapping to the CW system was not exact. Because of the lack of a coarse-graining step, the simulations were limited to a few clusters on a relatively small grid of size 100×100. Here we repeat Siddiqui's simulations on a much larger grid of size 490×490 and investigate the effects of noise reduction in some detail.

The model CW presented to simulate flow in a pipe network is basically *deterministic:* for any particular configuration of the radii in the network and initial conditions for the position of fluid-fluid interface, the model predicts a unique viscous fingering pattern. In the CW model, the pipe network is initially filled with viscous fluid, with an inviscid fluid entering at one vertex. The initial position of the fluid-fluid interface within the neighboring pipes is chosen randomly. The pressure is fixed at P_{input} inside the invading fluid. The circumference of the circular cell is held at $P=0$. The equation for the pressure, (2.3), is solved numerically. The fluid-fluid interface advances simultaneously in every pipe it occupies, with flow rate determined by Eq. (2.1) and velocity $\mathbf{v}=\mathbf{Q}/\pi r^2$. A time increment dt is chosen such that the interface closest to reaching a vertex arrives there. With the new boundary condition $P=P_{\text{input}}$ on the fluid-fluid interface, Eq. (2.3) is solved again, and the interface moves forward again. This process continues until the inviscid fluid reaches the outer boundary of the network.

Because numerical solutions of Eq. (2.3) introduce computational errors, there is some amount of noise inherent in simulations of the CW model. This numerical noise can cause a symmetry breaking in the flow pattern, much the same way fluctuations in the real system do. However, the noise enters in an uncontrolled fashion, and therefore its magnitude cannot be adjusted.

In DLA, tip splitting is caused by disorder in the growth process, and not by any disorder in the medium. It may be that in some sense the same is true of viscous fingering in a smooth Hele-Shaw cell.[4] It seems plausible that tip splitting is caused by some kind of noise or spontaneous fluctuations of the fluid-fluid interface, and not only by the microscopic roughness of the plates, especially because repeated experiments under virtually identical conditions in the same cell produce fingering patterns that appear to be uncorrelated.

It is also true that repeated viscous fingering experiments in the same porous medium produce different fingering patterns. That is, tip splitting and side branching seem to depend not only on the inhomogeneity of the medium, but also on some kind of symmetry-breaking noise at the fluid-fluid interface. Regardless of the actual source of this noise, it seems appropriate to consider a simulation which explicitly includes tunable noise terms.

One way to modify the CW model to include the effects of noise in a controlled fashion would be to add stochastic terms to Darcy's law. For example, we could choose one of two forms

$$\mathbf{v}=-k\nabla P(1+\alpha\xi)\ , \tag{3.1a}$$

or

$$\mathbf{v}=-k\nabla P+\alpha\xi\ . \tag{3.1b}$$

Here, α is an adjustable parameter and ξ a Gaussian random variable whose mean is 0 and whose standard deviation is unity. Noise of type (3.1a) might be called multiplicative noise, and noise of type (3.1b) additive noise. The parameter α tunes the noise in either case.

Instead of adding these noise terms to the CW model, we choose rather to use the more efficient IDLA model, with the addition of the noise-reduction technique. We then attempt to determine which type of noise, additive, or multiplicative, is the result.

One other important reason to investigate other ap-

proaches to simulation is computational efficiency. Because the CW model requires repeated solution of a partial-differential equation, it is computationally slow. A DLA-based model is by contrast much more efficient.

IV. NOISE REDUCTION

In DLA with noise reduction,[14–17] a perimeter site becomes a cluster site only after it has been hit by s random walkers, where s is an adjustable parameter. The original DLA model corresponds to $s=1$. Increasing s has a smoothing effect on the interface. We show here that noise reduction effectively controls interface velocity fluctuations according to the form in (3.1a), multiplicative noise. Noise reduction may be used with IDLA, but the argument given here applies equally to DLA or to other growth processes, i.e., the Eden model.[20]

Let p be the probability that a random walker will hit a given perimeter site i. Assume that p does not change very much over the time scale s/p, where time increases by one unit whenever a walker hits the cluster. The probability distribution $\mathcal{P}$ for the time t this site must wait before it is hit s times is

$$\mathcal{P}(t)=\left[\binom{t-1}{s-1}p^{s-1}(1-p)^{(t-1)-(s-1)}\right]p \ . \tag{4.1}$$

That is, there are $s-1$ hits in $t-1$ tries, then one hit on the tth try. In the Poisson limit that p is small and s is large, we obtain the approximation

$$\mathcal{P}_s(t)\cong\left[\frac{[(t-1)p]^{(s-1)}}{(s-1)!}e^{[(t-1)p]}\right]p \ . \tag{4.2a}$$

If we define the velocity of the interface at site i as $v=1/t$, then we can change variables and calculate properties of the distribution for v. That is,

$$\mathcal{P}_s(v)\cong\frac{p^s}{(s-1)!}\frac{e^{-p/v}}{v(s+1)} \ . \tag{4.2b}$$

Taking the first two moments of this distribution, we find

$$\langle v\rangle\cong\left[\frac{p}{s-1}\right]+\mathcal{O}\left[\frac{p^2}{s^2}\right]\cong p/s \ , \tag{4.3}$$

and

$$\langle(v-\langle v\rangle)^2\rangle^{1/2}=\frac{p}{s^{3/2}} \ . \tag{4.4}$$

If we do not consider higher moments of v, we can approximate $\mathcal{P}_s(v)$ as a Gaussian:

$$\mathcal{P}_s(v)=\frac{1}{\sqrt{2\pi\sigma}}e^{-(v-\langle v\rangle)^2\sqrt{s}/2\langle v\rangle} \ . \tag{4.5}$$

That is, the probability distribution for v is approximately a Gaussian centered at $\langle v\rangle=p/s$, with width $\langle v\rangle/\sqrt{s}$. To demonstrate that Eq. (4.2b) may be approximated by the Gaussian of Eq. (4.5), a comparison of the two distributions is shown in Fig. 4.

It is interesting to note that the fluctuations of v may be described by a stochastic equation,

$$v=\frac{p}{s}+\frac{p}{s^{3/2}}\xi$$
$$=\langle v\rangle\left[1+\frac{1}{\sqrt{s}}\xi\right] \ . \tag{4.6}$$

Equation (4.6) is similar in form to Eq. (3.1a), and corresponds to multiplicative noise. Thus adjusting the noise-reduction parameter s is roughly equivalent to adjusting the size of typical fluctuations of the interface velocity away from its mean value, which corresponds to the parameter α in (3.1a). The limit of s large corresponds to the no-noise limit because the size of a typical fluctuation goes to 0. Also, note that with multiplicative noise terms, fluctuations in the velocity are large where the velocity is large and small where the velocity is small.

The initial assumption that the hit probability p for a given site does not change much over time is, of course, not strictly valid. Rather, p is a function of time. As the cluster evolves, a perimeter site that was once at the outer tip of the cluster can become more and more screened, such that its p decreases and may even vanish. That means that the small-velocity (long-waiting-time) part of the velocity distribution is inflated by the approxi-

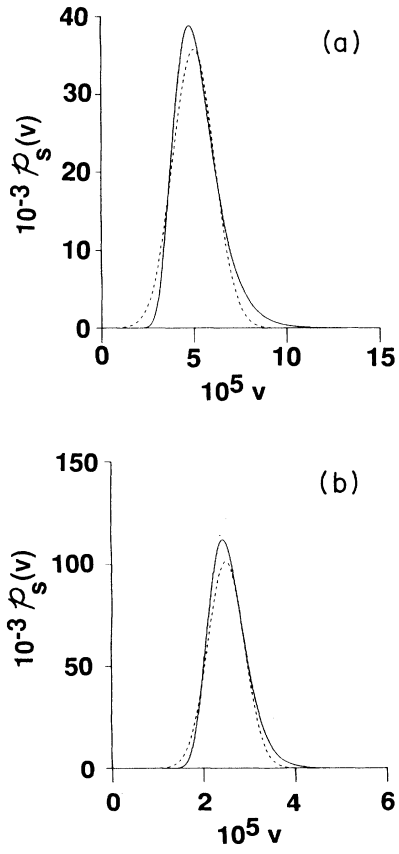

FIG. 4. A comparison of the functions defined in Eqs. (4.2b) (solid line) and (4.5) (dashed line). In (a), $p=0.001$ and $s=20$, and in (b) $p=0.001$ and $s=40$. To the extent that the solid and dashed curves overlap, the approximation discussed in the text is correct.

mation that p is constant. We expect that this approximation does not change the scaling properties of the mean and width of the distribution.

V. RESULTS

Shown in Fig. 5 are three IDLA clusters which were generated with noise reduction $s=50$ and $\lambda=0$, 0.5, and 0.99. Small clusters (mass of 1000) are shown here for comparison with the CW experimental and simulation results. The $\lambda=0$ cluster is strongly cross shaped, with a gradual transition to more DLA-like clusters for larger λ. This result is in qualitative agreement with the CW experiments and simulations. Because IDLA models flow in a pore-pipe network, and CW's experiments are with a pipe network, detailed quantitative comparison would be inappropriate.

In Fig. 6 are displayed two clusters generated by the IDLA algorithm on the *same* inhomogeneous pipe network, which has $\lambda=0.25$. The clusters were grown with no noise reduction, that is, $s=1$, and are different from each other only because different random-number seeds were used to start the random walks. Although the two clusters appear somewhat similar in overall shape, their detailed forms differ from the earliest stages of growth. Tip splitting and the formation of side branches are clearly influenced both by the disorder in the permeability of the medium and by the noise associated with the growth process.

How do these two sources of noise interact? In Fig. 7 we show two pairs of IDLA clusters where each pair was grown on the same disordered pipe network. The first cluster in each pair [7(a) and 7(c)] has $s=1$, while the

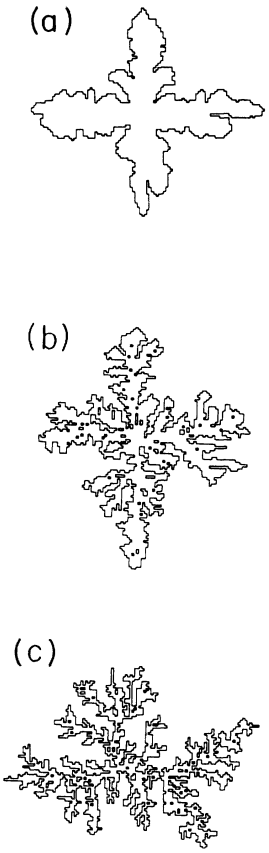

FIG. 5. IDLA simulations for (a) $\lambda=0$, (b) $\lambda=0.5$, and (c) $\lambda=0.99$, all with $s=50$. For comparison, these clusters are of approximately the same mass (1000) as those produced by the CW model in Fig. 1 of Ref. 3. The similarity between these clusters and those produced by the CW model suggests that the CW model is roughly equivalent to IDLA in the large- s limit. Note that part (a), homogeneous DLA, is equivalent to the model studied in Ref. 4.

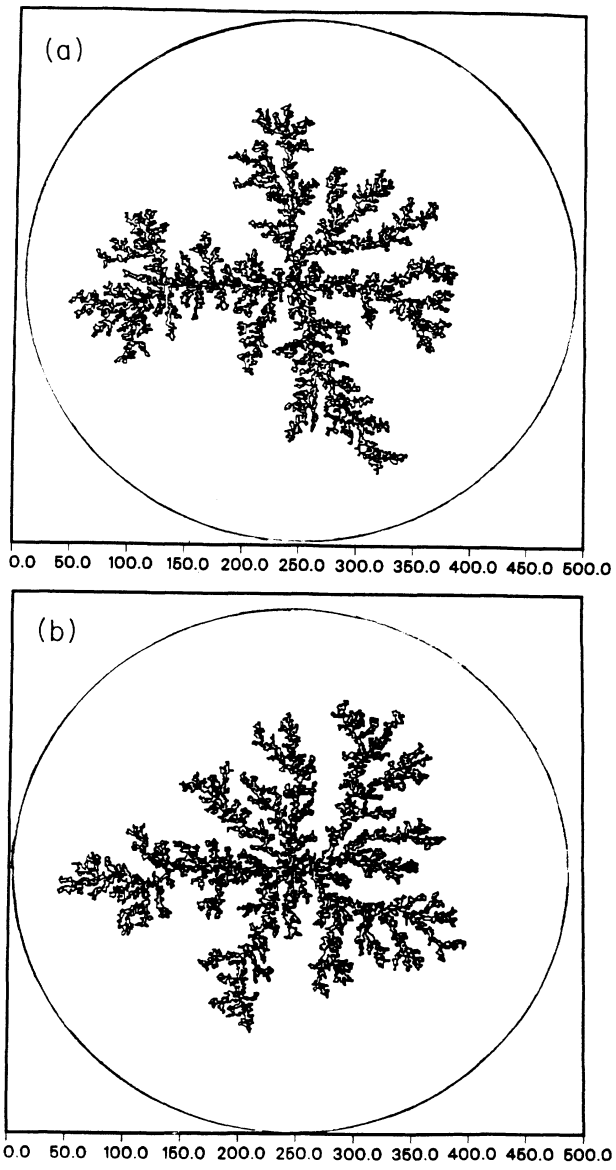

FIG. 6. Two IDLA simulations for $\lambda=0.25$, $s=1$, made with the identical disordered pipe network, but with random walks initiated with different random number seeds. These two clusters represent two different outcomes of a viscous fingering experiment in the same porous medium.

second cluster in each pair [7(b) and 7(d)] has $s=10$. For a low value of the disorder parameter λ, noise reduction has much the same effect as it does in regular DLA on a square lattice. The finger width increases, and the fingers grow predominantly along straight lines, giving rise to a dendritic morphology. But for a higher value of λ we find an entirely different result. Even with noise reduction, the cluster appears to take on a shape much like that of regular DLA.

The IDLA model is unique in that it probes systems with noise or fluctuations in both the permeability and in the growth process itself. Thus we can use it to map out a "morphology phase diagram," which is shown in schematic form in Fig. 8. On the horizontal axis we plot λ, which measures the disorder in the permeability. On the vertical axis we plot $1/\sqrt{s}$, the quantity that gives the magnitude of typical fluctuations in the velocity. For instance, if $s=100$, then $1/\sqrt{s}=0.1$, and the interface velocity has fluctuations which are typically 10% of the average velocity. Thus $1/\sqrt{s}$ is a quantity which characterizes the noise in the growth process. The CW model, in principle, corresponds to the $s\to\infty$ limit; that is, to the points along the horizontal axis of Fig. 8. Points along the vertical axis have $\lambda=0$ and correspond to DLA

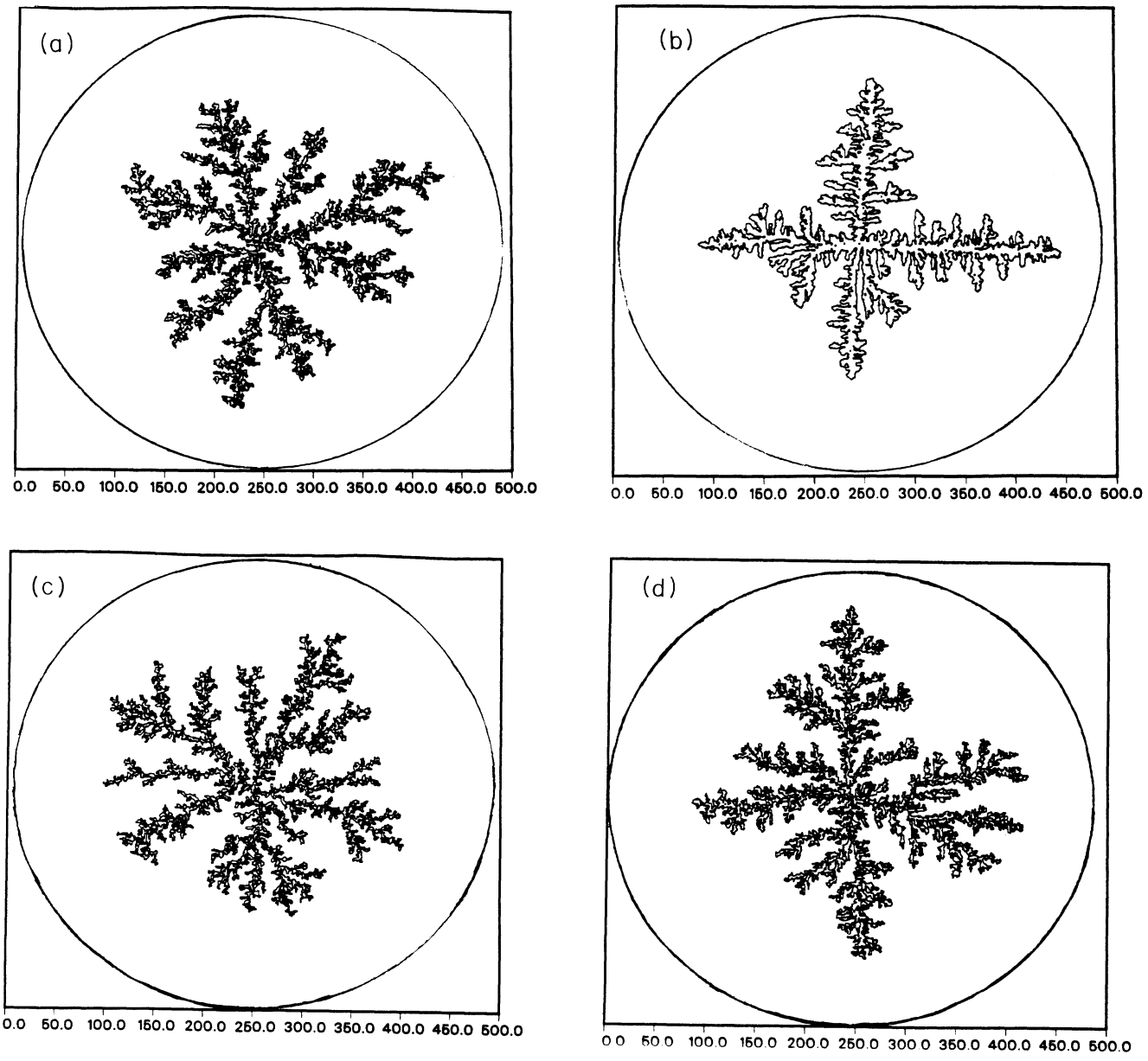

FIG. 7. IDLA simulations of two very weakly inhomogeneous systems—(a) $\lambda=0.1$, $s=1$; (b) $\lambda=0.1$, $s=10$—and of two strongly inhomogeneous systems—(c) $\lambda=0.9$, $s=1$; and (d) $\lambda=0.9$, $s=10$. Note that only the weakly inhomogeneous system with large noise reduction s [case (b)] displays dendritic morphology.

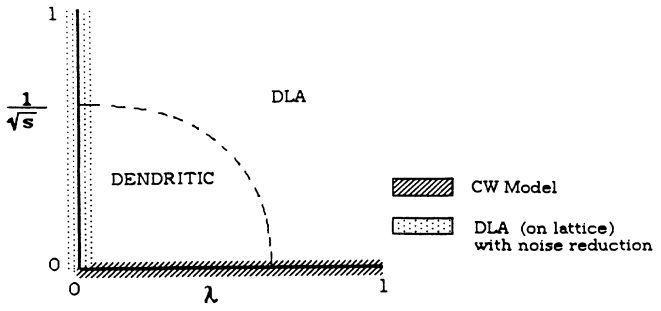

FIG. 8. A "morphology phase diagram." The horizontal axis variable λ controls the strength of the inhomogeneity in the permeability, while the vertical axis variable $1/\sqrt{s}$ controls the noise in the growth process. Several special points on the diagram are $\lambda=0$, $1/\sqrt{s}=1$ (normal homogeneous DLA); $\lambda=0$, $0<1/\sqrt{s}<1$ (DLA with noise reduction, shown in dotted area along y axis); $0<\lambda<1$, $1/\sqrt{s}=0$ (CW model, shown in hatched area along x axis); $\lambda=0$, $1/\sqrt{s}=0$ (fourfold-symmetric dendrite). The position of the transition line is based on data from finite clusters and therefore is schematic.

with DBM boundary conditions and noise reduction. The special point ($\lambda=0$, $1/\sqrt{s}=0$) corresponds to a growth process with no noise in a perfectly homogeneous square lattice, which at least, in principle, would produce a fourfold-symmetric dendritic structure.

Moving away from the special points at the origin, we find clusters which appear to be disordered dendrites; that is, dendritic shapes with side branches of random lengths. At points yet further from the origin, we find dendrites which are more disordered with fingerlike side branches, and finally at a greater distance we find clusters which are DLA-like. The transition from dendritic to DLA-like morphology appears to be smooth. For this reason, the transition line plotted in Fig. 8 is schematic.

How can we quantify the transition from dendritic to DLA-like morphology? To try to answer this question, we generated a large number of clusters with noise reduction $s=4$ and λ in the range 0.3–0.7, with 30 clusters at each λ value. These clusters fall along a horizontal line across the morphology phase diagram, such that for small λ the clusters appear dendritic, and for large λ they appear DLA-like.

One way to quantify the transition from dendritic to DLA-like would be to measure the fractal dimensions of the clusters. One might expect that the dendritic clusters should have fractal dimension d_f of about 1.5,[4] while the DLA-like clusters should have d_f closer to 1.7.[10] Unfortunately, evaluation of the limiting fractal dimension of our IDLA clusters is somewhat problematic because the clusters are probably not large enough to be in the asymptotic regime, as their typical mass is 15 000–20 000. An even greater difficulty, however, is that there are extremely important edge effects from the circular outer boundary. We calculate the function $M(r)$, the mass in a circle of radius r, and from log-log plots of $M(r)$ versus r we find the slope d_f in the range 1.6–1.7 for all our clusters, both DLA-like and dendritic. It is not clear whether this finding reflects something important about the morphology transition or if it is just an artifact of the boundary conditions.

Perhaps a better way to characterize the transition is to look at the properties of the angular mass distribution function $m(\theta)$, where $m(\theta)d\theta$ is the fraction of the total mass of the cluster in the angular wedge between θ and $\theta+d\theta$. Here angles are figured from the center of the cluster, which we take to be the position of the seed, with $\theta=0$ along one of the axes of the square lattice. One expects that for a dendritic cluster, $m(\theta)$ should be sharply peaked at the four angles which correspond to the protruding arms of the cluster. Consider the Fourier series for $m(\theta)$,

$$m(\theta)=\frac{a_0}{2}+\sum_{j=1}^{\infty}a_j\cos(j\theta)+\sum_{j}^{\infty}b_j\sin(j\theta)\ . \tag{5.1}$$

We take $c_4=\pi[(a_4)^2+(b_4)^2]^{1/2}$ as a measure of the dendritic nature of a cluster. In practice, it is not necessary to calculate the function $m(\theta)$ explicitly. Rather, we can calculate directly:

$$\begin{aligned}a_4&=\frac{1}{\pi}\int d\theta\, m(\theta)\cos(4\theta)\\&=\frac{1}{M\pi}\int d\theta\left[\sum_{i=1}^{M}\delta(\theta-\theta_i)\right]\cos(4\theta)\ .\end{aligned} \tag{5.2}$$

Here, M is the total number of particles (mass) in the cluster and θ_i refers to the angular position of the ith particle.

We calculated c_4 for 30 DLA (that is, $\lambda=0$) clusters of mass 15 000–20 000 and found an average value $\langle c_4\rangle=0.19$. (This value probably depends on cluster size.) A plot of c_4 versus λ for fixed noise reduction $s=4$ is shown in Fig. 9. As the clusters cross from dendritic to DLA-like, c_4 drops dramatically towards its DLA value. Thus we conjecture that c_4 could be an order parameter for the transition.

One important worry is that our data are based on relatively small clusters. For larger clusters, the position of the transition in the morphology phase diagram would be

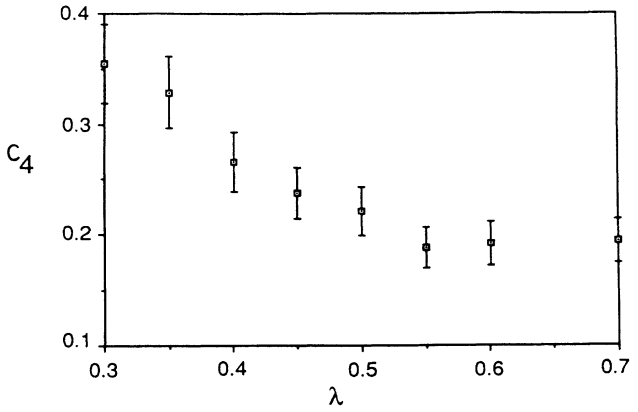

FIG. 9. A plot of c_4 vs λ, where c_4 is a measure of the fourfold symmetry of the cluster. We conjecture that c_4 may be a suitable order parameter for the morphology phase transition.

altered since the lattice anisotropy gains importance with lattice size. In fact, there is evidence that DLA on a square lattice looks somewhat dendritic on a large scale for clusters of mass larger than 10^6.[21] That is, in the infinite-mass limit, IDLA might always produce dendritic clusters, regardless of the values of s and λ. However, given the data we have, we conclude that for finite-mass clusters both noise associated with the growth process and noise associated with the disordered medium can drive the growth process towards a DLA-like structure.

One other measurement of viscous fingering systems is their area-sweep efficiency (ASE), which is the ratio at breakthrough of the volume of displacing fluid over the total volume of viscous fluid which was originally in the system at time 0. The ASE is a measure of the efficiency of the oil-recovery process, and is normally determined from a quarter-five-spot simulation. This quantity is commonly used by petroleum engineers. Because it is a measurement of the density of a fractal structure, the ASE is not constant but decreases with increasing system size. However, by holding the system size fixed, we can determine the ASE's general dependence on λ. We generated quarter-five-spot clusters with $s=1$ and several values of λ; one such cluster is shown in Fig. 10(a). In Fig. 10(b) the ASE is shown as a function of λ. Each point on the graph represents an average over 10 clusters. It appears that the ASE increases weakly and monotonically with λ for $s=1$. This qualitative result of our model could be compared with viscous fingering experiments in two-dimensional porous-medium Plexiglas® models.

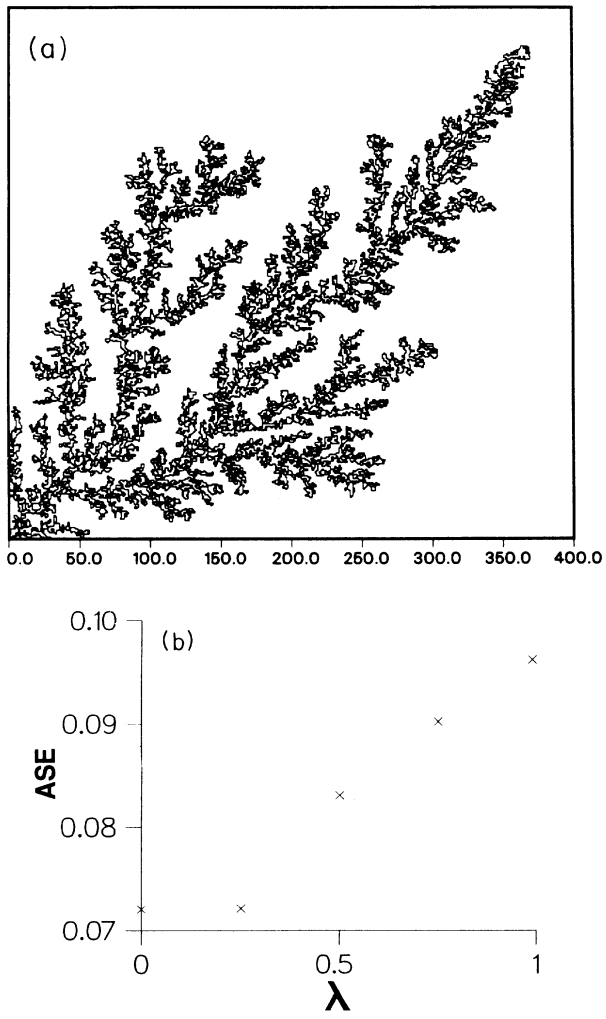

FIG. 10. (a) An inhomogeneous DLA cluster with $\lambda=0.5$, $s=1$, in the quarter-five-spot geometry. (b) The area-sweep efficiency (ASE) as a function of λ with $s=1$, determined from clusters such as (a). Each point represents an average over 10 clusters.

VI. SUMMARY

We have demonstrated that the IDLA model can be used to simulate viscous fingering in a medium with inhomogeneous permeability and homogeneous porosity. We determined that fluctuations in a DLA-based growth process may be tuned by means of noise reduction, and that fluctuations in the velocity of the moving interface are multiplicative in form. That is, deviations from the mean velocity are proportional to the mean velocity with proportionality factor $1/\sqrt{s}$, where s is the noise-reduction parameter.

We used the IDLA model to simulate viscous fingering in a medium which consists of a pipe-pore square-lattice network in which all pores have equal volume and the pipes have negligible volume. The pipe radii are chosen randomly from a probability distribution function with tunable width λ. By varying both λ and s, we mapped out a morphology phase diagram which shows a gradual transition from dendritic to DLA-like cluster shapes. A possible order parameter for this transition was defined and calculated. In future work, we hope to find experimental data which might allow us to determine the actual source of interface velocity fluctuations in viscous fingering.

Siddiqui and Sahimi[13] recently proposed a DLA-based algorithm for modeling viscous fingering of fluids with finite-mobility ratio, and methods have been proposed for including the effects of surface tension.[19,22] With the IDLA model we can add inhomogeneous permeability, and noise reduction allows us to adjust the magnitude of interface velocity fluctuations. With all these tools, it appears likely that DLA-based simulations for realistic fluid-flow problems involving immiscible fluid flow—including those encountered in petroleum-reservoir simulation—may soon be a reality.

We also hope to apply DLA-based methods to simulating dendritic crystal growth. Here, in particular, there may be a need for large-scale three-dimensional simulations which might not be feasible with non-DLA-based methods. Such simulations might be used to predict morphology as a function of the physical parameters in the crystal growth process.

ACKNOWLEDGMENTS

We would like to thank P. Meakin, F. Leyvraz, and G. Huber for helpful discussions and S. Milošević for impor-

tant collaboration in the early stages of this work. We would also like to thank Professor O. Preining and Dozent W. Kratky of the University of Vienna for providing research facilities during the completion of this work. We thank the Boston University Academic Computing Center for generously providing necessary computer resources. This work was supported by the U.S. National Science Foundation, the Office of Naval Research, the National Aeronautics and Space Administration, and the Link Foundation.

APPENDIX: THE CONNECTION BETWEEN IDLA AND TWO-FLUID DISPLACEMENT

In this appendix we trace the connection between IDLA and viscous fingering in inhomogeneous media in two dimensions.[11,19,23]

First, we review the connection between the original DLA model and two-fluid displacement in homogeneous media in two dimensions. Consider a DLA system where a random walker is released from a random point on a circular boundary far from the cluster and is allowed to diffuse until it either returns to the boundary (and is destroyed) or hits a cluster site (and sticks). Here we are considering DBM-type boundary conditions.[8] Let $\rho(\mathbf{x},t)$ be the probability density of a walk released from an unknown point on the circular boundary at time $t=0$. The diffusion equation for $\rho(x,t)$ is

$$\frac{\partial\rho}{\partial t}=\tfrac{1}{4}\nabla^2\rho\ , \tag{A1}$$

where the walker makes one step per unit time. In this appendix, continuum operators represent their discretized analogs. Boundary conditions on $\rho(x,t)$ are

$$\rho(x,0)=\begin{cases}\text{const} & \text{for } x\in\text{circular boundary},\\ 0 & \text{otherwise},\end{cases} \tag{A2a}$$

$$\rho(x,t)=0 \quad \text{for } x\in\text{circular boundary};\ t>0\ , \tag{A2b}$$

$$\rho(x,t)=0 \quad \text{on cluster sites for all } t\ . \tag{A2c}$$

Let $G(x)$ be defined as the time integral of $\rho(x,t)$,

$$G(x)\equiv\sum_{t=0}^{\infty}\rho(x,t)\ . \tag{A3}$$

Boundary conditions on $G(x)$ follow from (A2):

$$G(x)=\begin{cases}\text{const} & \text{for } x\in\text{circular boundary},\\ 0 & \text{for } x\in \text{ cluster}\ .\end{cases} \tag{A4}$$

Taking the Laplacian of $G(x)$, we find

$$\begin{aligned}\nabla^2G(x)&=\nabla^2\left[\sum_{t=0}^{\infty}\rho(x,t)\right]\\ &=\sum_{t=0}^{\infty}4\frac{\partial\rho}{\partial t}(x,t)\\ &\cong 4\int_0^{\infty}\frac{\partial\rho}{\partial t}(x,t)dt\\ &=4[\rho(x,\infty)-\rho(x,0)]\\ &=0 \quad \text{for } x \text{ not on cluster or outer boundary}\ .\end{aligned} \tag{A5}$$

Thus $G(x)$ plays the role of the pressure in obeying the Laplace equation.

It remains to show that the cluster boundary advances according to Darcy's law (2.1). Take x_i to be a site adjacent to a cluster site x_j. The probability for a walker to land on x_i at time t and then step onto x_j at time $t+1$ is the growth probability p_{grow} of x_i at time t,

$$p_{\text{grow}}(x_i,t)=\tfrac{1}{4}\rho(x_i,t)\ . \tag{A6a}$$

Integrating over all time, we find the total growth probability $\tilde{p}_{\text{grow}}$,

$$\tilde{p}_{\text{grow}}(x_i)=\sum_{t=0}^{\infty}\tfrac{1}{4}\rho(x_i,t)=\tfrac{1}{4}G(x_i)\ . \tag{A6b}$$

From (A4), $G(x_j)=0$ because x_j is a cluster site; thus we may write

$$\tilde{p}_{\text{grow}}(x_i)=\tfrac{1}{4}G(x_i)=\tfrac{1}{4}[G(x_i)-G(x_j)]=\frac{\nabla G(x_i)}{4}\ . \tag{A7}$$

We may interpret $\tilde{p}_{\text{grow}}(x_i)$ as the analog of the interface velocity at site x_i; then Eq. (A7) takes the same form as Darcy's law.

Thus we have shown that the DLA model is like viscous fingering in that there is a function $G(x)$ which plays the role of P in obeying the Laplace equation and Dirichlet boundary conditions. The growth probability $\tilde{p}_{\text{grow}}$ plays the role of an interface velocity in obeying Darcy's law.

Now we turn to IDLA and demonstrate its connection to viscous fingering in inhomogeneous media in two dimensions. For our system the permeability k has been arbitrarily fixed on each bond of a square lattice, normalized such that the largest k is $1/z$. Everything is the same as in DLA, except that the random walker is biased toward high-permeability bonds and chooses its steps according to Eq. (2.10). The probability density $\rho(x,t)$ and the time-integrated probability density $G(x)$ both obey the same boundary conditions as in the original DLA system described above. However, $\rho(x,t)$ now obeys a different diffusion equation,

$$\frac{\partial\rho}{\partial t}=\nabla\cdot(k\nabla\rho)\ , \tag{A8}$$

instead of (A1). Now we form the quantity

$$\begin{aligned}\nabla\cdot[k\nabla G(x)]&=\nabla\cdot\left[\sum_{t=0}^{\infty}k\nabla\rho(x,t)\right]\\ &=\int_0^{\infty}\frac{\partial\rho}{\partial t}dt\\ &=\rho(x,\infty)-\rho(x,0)\\ &=0\ ,\end{aligned} \tag{A9}$$

for x neither a cluster nor a boundary site. Thus, $G(x)$ plays the role of the pressure P in the sense that (A9) has the form of (2.3).

If x_j is a cluster site and x_i is an adjacent empty site, then the growth probability at x_i at time t is

$$p_{\text{grow}}(x_i,t)=\rho(x_i,t)k_{ij}\ , \tag{A10}$$

where k_{ij} is the normalized permeability of the bond between sites i and j. Integrated over the lifetime of the walker, the growth probability is

$$\begin{aligned}\tilde{p}_{\text{grow}}(x_i) &= \sum_{t=0}^{\infty} \rho(x_i,t)k_{ij} \\ &= G(x_i)k_{ij} \\ &= k_{ij}[G(x_i)-G(x_j)] \\ &= k\nabla G(x)\ . \end{aligned} \tag{A11}$$

We again interpret $\tilde{p}_{\text{grow}}$ as the analog of the interface velocity at x_i and we see that it has the same form as Eq. (2.1).

Hence the IDLA model is like viscous fingering in inhomogeneous media in that $G(x)$ plays the role of P in obeying Eq. (2.4), and the growth probability $\tilde{p}_{\text{grow}}$ plays the role of the interface velocity in obeying Darcy's law. Thus IDLA may be used to model fluid flow in inhomogeneous media.

[1]P. Meakin, Phys. Rev. A **36**, 2833 (1987).

[2]R. Lenormand and C. Zarcone, Phys. Rev. Lett. **54**, 2226 (1985).

[3]J. Chen and D. Wilkinson, Phys. Rev. Lett. **55**, 1892 (1985).

[4]J. Nittmann, G. Daccord, and H. E. Stanley, Nature (London) **314**, 141 (1985).

[5]G. Daccord, J. Nittmann, and H. E. Stanley, Phys. Rev. Lett. **56**, 336 (1986).

[6]K. J. Maløy, J. Feder, and T. Jøssang, Phys. Rev. Lett. **55**, 2688 (1985); U. Oxaal, M. Murat, F. Boger, A. Aharony, J. Feder, and T. Jøssang, Nature (London) **329**, 32 (1987); M. Murat and A. Aharony, Phys. Rev. Lett. **57**, 1875 (1986); P. Meakin, M. Murat, A. Aharony, J. Feder, and T. Jøssang, Physica A **155**, 1 (1989).

[7]M. Sahimi and H. Siddiqui, J. Phys. A **20**, L89 (1987).

[8]L. Niemeyer, L. Pietronero, and H. J. Wiesmann, Phys. Rev. Lett. **52**, 1033 (1984).

[9]F. Family, D. Platt, and T. Vicsek, J. Phys. A **20**, L1177 (1987); J. Nittmann and H. E. Stanley, *ibid.* **20**, L1185 (1987); **20**, L981 (1987).

[10]T. A. Witten and L. M. Sander, Phys. Rev. Lett. **47**, 1400 (1981).

[11]L. Paterson, Phys. Rev. Lett. **52**, 1621 (1984); L. Paterson, J. Fluid Mech. **113**, 513 (1981).

[12]L. Paterson, J. Phys. A **20**, 2197 (1987).

[13]H. Siddiqui and M. Sahimi, Chem. Eng. Sci. (to be published).

[14]C. Tang, Phys. Rev. A **31**, 1977 (1985).

[15]J. Nittmann and H. E. Stanley, Nature (London) **321**, 663 (1986).

[16]J. Kertesz and T. Vicsek, J. Phys. A **19**, L257 (1986).

[17]P. Meakin, Phys. Rev. A **36**, 325 (1987); J. P. Eckmann, P. Meakin, I. Procaccia, and R. Zeitak, *ibid.* **39**, 3185 (1989), and references contained therein.

[18]S. Havlin and D. Ben-Avraham, Adv. Phys. **36**, 695 (1987); see, e.g., D. C. Hong, H. E. Stanley, A. Coniglio, and A. Bunde, Phys. Rev. B **33**, 4564 (1986).

[19]L. Kadanoff, J. Stat. Phys. **39**, 267 (1985).

[20]M. Eden, in *Proceedings of the Fourth Berkeley Symposium on Mathematical Statistics and Probability,* edited by J. Neyman (University California Press, Berkeley, 1961), Vol. IV, p. 223.

[21]P. Meakin, R. C. Ball, P. Ramanlal, and L. M. Sander, Phys. Rev. A **35**, 5233 (1987).

[22]T. Vicsek, Phys. Rev. Lett. **53**, 2281 (1986).

[23]The argument in Eqs. (A1)–(A7) was pointed out to us by F. Leyvraz (private communication).